

Assessing the Impact of Post-Quantum Digital Signature Algorithms on Blockchains

Alison Gonçalves Schemitt

PUCRS

Porto Alegre, Brazil

alison.schemitt@edu.pucrs.br

Henrique Fan da Silva

UNIPAMPA

Alegrete, Brazil

henriquefan.aluno@unipampa.edu.br

Roben Castagna Lunardi

IFRS and PUCRS

Porto Alegre, Brazil

roben.lunardi@zonanorte.ifrs.edu.br

Diego Kreutz

UNIPAMPA

Alegrete, Brazil

diegokreutz@unipampa.edu.br

Rodrigo Brandão Mansilha

UNIPAMPA

Alegrete, Brazil

mansilha@unipampa.edu.br

Avelino Francisco Zorzo

PUCRS

Porto Alegre, Brazil

avelino.zorzo@pucrs.br

Abstract—The advent of quantum computing threatens the security of traditional encryption algorithms, motivating the development of post-quantum cryptography (PQC). In 2024, the National Institute of Standards and Technology (NIST) standardized several PQC algorithms, marking an important milestone in the transition toward quantum-resistant security. Blockchain systems fundamentally rely on cryptographic primitives to guarantee data integrity and transaction authenticity. However, widely used algorithms such as ECDSA, employed in Bitcoin, Ethereum, and other networks, are vulnerable to quantum attacks. Although adopting PQC is essential for long-term security, its computational overhead in blockchain environments remains largely unexplored. In this work, we propose a methodology for benchmarking both PQC and traditional cryptographic algorithms in blockchain contexts. We measure signature generation and verification times across diverse computational environments and simulate their impact at scale. Our evaluation focuses on PQC digital signature schemes (ML-DSA, Dilithium, Falcon, Mayo, SLH-DSA, SPHINCS+, and Cross) across security levels 1 to 5, comparing them to ECDSA, the current standard in Bitcoin and Ethereum. Our results indicate that PQC algorithms introduce only minor performance overhead at security level 1, while in some scenarios they significantly outperform ECDSA at higher security levels. For instance, ML-DSA achieves a verification time of 0.14 ms on an ARM-based laptop at level 5, compared to 0.88 ms for ECDSA. We also provide an open-source implementation to ensure reproducibility and encourage further research.

Index Terms—Blockchain, Post-Quantum Cryptography, Digital Signatures, ML-DSA, SLH-DSA, Falcon

I. INTRODUCTION

In recent years, research and development in quantum computing have advanced significantly, leveraging quantum-mechanical principles to tackle computationally intractable problems [1]. Quantum computers can efficiently execute

This study was partially funded by the Conselho Nacional de Desenvolvimento Científico e Tecnológico (CNPq) – Brazil, by the Brazilian National Research and Education Network (RNP) under the Iliada Project, and by the Fundação de Amparo à Pesquisa do Estado do Rio Grande do Sul (FAPERGS) through grant no. 22/2551-0000841-0 (INOVA-RS). In addition, Roben Lunardi is supported by FAPERGS and IFRS, and holds a postdoctoral fellowship from CAPES (PIP/CAPES).

Shor's algorithm [2], which poses a critical threat to cryptographic systems that rely on widely deployed algorithms such as RSA and ECDSA.

To address this challenge, the National Institute of Standards and Technology (NIST) initiated a process in 2016 to standardize post-quantum cryptography (PQC) algorithms. This effort has so far culminated in the approval of two digital signature schemes: FIPS 204, the Module-Lattice-Based Digital Signature Algorithm (ML-DSA) [3], formerly known as Dilithium; and FIPS 205, the Stateless Hash-Based Digital Signature Algorithm (SLH-DSA) [4], formerly SPHINCS+. In addition, the Falcon algorithm [5] has been approved and will be standardized as FIPS 206, the Fast-Fourier Transform over NTRU-Lattice-Based Digital Signature Algorithm (FN-DSA).

Beyond these standardized schemes, we also consider Cross [6] and Mayo [7], two candidate algorithms from the additional rounds of the NIST signature standardization process. Despite this progress, the performance and practicality of these algorithms across heterogeneous hardware platforms, software stacks, and application environments remain insufficiently explored.

Blockchains rely heavily on cryptography to ensure both integrity and authenticity. The ECDSA algorithm, widely adopted in networks such as Bitcoin and Ethereum, has been shown to be particularly vulnerable to quantum attacks [2], [8]. This vulnerability highlights the urgent need to migrate blockchain systems toward post-quantum cryptographic (PQC) alternatives. Although the adoption of PQC algorithms is essential for long-term security, their computational overhead in blockchain environments remains insufficiently explored [9], especially when compared to evaluations conducted in other domains [10]–[14].

We aim to assess the performance impact on blockchain systems when migrating from traditional digital signature algorithms (e.g., ECDSA, RSA) to PQC alternatives (e.g., ML-DSA, SLH-DSA). This paper makes three main contributions:

- **Methodology:** We propose a clear and reproducible

TABLE I
COMPARISON AMONG THIS AND RELATED WORKS.

Ref.	Traditional	ECDSA	Post-Quantum				Cross	CPU Architecture		Blockchain focus
			ML-DSA (Dilithium)	Falcon	Mayo	SLH-DSA (SPHINCS+)		X64	ARM	
This work	✓		✓	✓		✓	✓	✓	✓	✓
[9]	✓		✓	✗		✓	✗	✓	✗	✓
[10]	✓		✓	✗		✓	✗	✓	✗	✗
[11]	✓		✓	✗		✓	✗	✓	✓	✗
[12]	✓		✓	✗	✗	✗	✗	✓	✗	✗
[13]	✓		✓	✓		✓	✗	✓	✓	✗
[14]	✗		✓	✓	✗	✓	✗	✓	✓	✗

methodology that combines (i) algorithm benchmarking to evaluate isolated performance for three fundamental operations (key pair generation, signing, and signature verification), and (ii) large-scale simulation to assess the impact of these operations on blockchain systems. To ensure transparency and foster further research, we provide a public repository with all implementations and datasets.

- **Empirical Evaluation:** We present an extensive empirical evaluation comprising more than 31,000 runs across three computational environments (two laptops and one desktop), covering two CPU architectures (x64 and ARM) and two operating systems (macOS and Linux). Our analysis includes seven algorithm families, comprising 62 implementations representing all NIST-defined security levels [15] (Levels 1–3 and 5, since no proposals exist for Level 4), providing a comprehensive performance characterization.
- **Findings:** Our results demonstrate the practical feasibility of integrating PQC algorithms into blockchain systems. The evidence indicates that PQC can be adopted without prohibitive overhead, while also strengthening the long-term security of blockchain networks.

This paper is organized as follows. Section II discusses related work and identifies gaps our research addresses. Section III describes our methodology and experimental setup. Section IV analyzes the findings, and Section V concludes with future research directions.

II. RELATED WORKS

The cryptography community has extensively discussed the standardization of Post-Quantum Cryptography (PQC) algorithms in recent years. Table I summarizes representative works that evaluate these algorithms. The PQC algorithms studied in these papers were either finalists or selected as NIST standards. In addition, works such as [9]–[13] also provide comparisons between PQC algorithms and traditional digital signature algorithms.

These studies primarily assess the performance of signature generation and verification. Among them, only [9] explicitly considers blockchain. This work analyzes real-time transaction payloads from a local blockchain and applies them to create and verify signatures using PQC algorithms and ECDSA.

The studies in [10], [12] compare traditional algorithms (e.g., ECDSA) with PQC algorithms (e.g., ML-DSA) across different security levels. The work in [12] further evaluates versions with and without hardware optimizations (AVX2). Both studies show that ECDSA achieves the best performance among traditional algorithms, while ML-DSA consistently performs best among PQC alternatives.

The works in [13], [14] examine PQC algorithms in the context of IoT devices and general-purpose computers, with [13] also including comparisons with traditional algorithms. Both conclude with recommendations on algorithm suitability depending on the target device type (desktop, laptop, or IoT). The study in [11] evaluates PQC algorithms in the context of smart vehicles (V2X) and concludes that, despite the good performance of some algorithms, none of the tested schemes fully meet the strict requirements of V2X systems.

Overall, related work highlights that ML-DSA performs comparably to, and in some cases better than, traditional algorithms such as ECDSA, although with higher memory consumption [9], [12]. At the same time, results show that in constrained environments such as IoT, PQC algorithms may not satisfy all system requirements, particularly with respect to key storage and resource limitations [11].

Our work differs by directly comparing standardized and finalist NIST PQC algorithms with ECDSA, which remains the dominant digital signature scheme in blockchain systems. Unlike prior studies, we specifically analyze the performance impact of migrating from traditional to PQC algorithms on block verification in blockchain environments.

III. PROPOSED EVALUATION METHODOLOGY

This section presents our methodology, implementation details, and experimental setup.

A. Workflow

Figure 1 illustrates the methodological workflow, which is structured into three main components: (1) Inputs, (2) Processing, and (3) Outputs.

The inputs consist of cryptographic algorithms, either traditional or post-quantum (PQC), along with their configurable parameters. We also define experimental parameters, such as the number of repetitions, to ensure statistically reliable results

TABLE II

ANALYZED ALGORITHMS. AMONG THE EVALUATED ALGORITHMS, ONLY TWO SUPPORT SECURITY LEVEL 2, AND NONE ARE AVAILABLE FOR LEVEL 4.

PQC?	#	Algorithm (16)	Variants (46)				
			Level 1 (14)	Level 2 (2)	Level 3 (14)	Level 4 (0)	Level 5 (16)
Yes	1	ECDSA	P-256	—	P-384	—	P-521
	2	ML-DSA*	—	ML-DSA-44	ML-DSA-65	—	ML-DSA-87
	3	Dilithium*	—	Dilithium2	Dilithium3	—	Dilithium5
	4	Falcon	Falcon-512	—	—	—	Falcon-1024
	5	Falcon-padded	Falcon-padded-512	—	—	—	Falcon-padded-1024
	6	Mayo	MAYO-2	—	MAYO-3	—	MAYO-5
	7	SPHINCS+-SHA-s	SHA2-128s-simple	—	SHA2-192s-simple	—	SHA2-256s- simple
	8	SPHINCS+-SHA-f	SHA2-128f-simple	—	SHA2-192f-simple	—	SHA2-256f-simple
	9	SPHINCS+-SHAKE-s	SHAKE-128s-simple	—	SHAKE-192s-simple	—	SHAKE-256s-simple
	10	SPHINCS+-SHAKE-f	SHAKE-128f-simple	—	SHAKE-192f-simple	—	SHAKE-256f-simple
	11	Cross-rsdp-small	Cross-rsdp-128-small	—	Cross-rsdp-192-small	—	Cross-rsdp-256-small
	12	Cross-rsdpg-small	Cross-rsdpg-128-small	—	Cross-rsdpg-192-small	—	Cross-rsdpg-256-small
	13	Cross-rsdp-balanced	Cross-rsdp-128-balanced	—	Cross-rsdp-192-balanced	—	Cross-rsdp-256-balanced
	14	Cross-rsdpg-balanced	Cross-rsdpg-128-balanced	—	Cross-rsdpg-192-balanced	—	Cross-rsdpg-256-balanced
	15	Cross-rsdp-fast	Cross-rsdp-128-fast	—	Cross-rsdp-192-fast	—	Cross-rsdp-256-fast
	16	Cross-rsdpg-fast	Cross-rsdpg-128-fast	—	Cross-rsdpg-192-fast	—	Cross-rsdpg-256-fast

*Includes legacy (pre-standardization) implementations and current NIST-standardized.

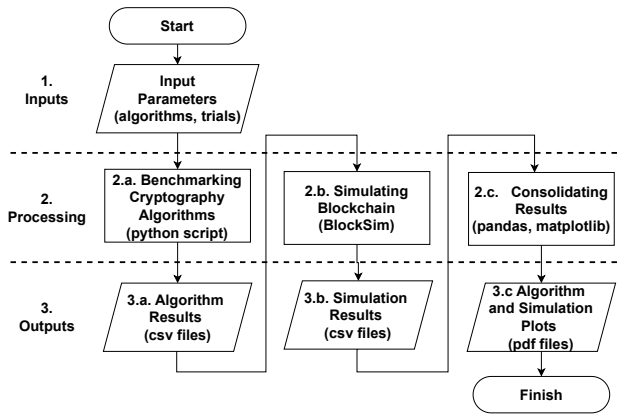


Fig. 1. Methodological workflow.

in both the algorithm benchmarking and blockchain simulation stages.

The processing pipeline is organized into three sequential stages. In the first stage (2.a), focused on algorithm benchmarking, cryptographic algorithms are executed to measure key performance indicators, namely key generation, signing, and verification. These baseline measurements are then used in the second stage (2.b), the blockchain simulation, where the behavior of the algorithms is modeled during block verification in a distributed ledger environment. In the final stage (2.c), result synthesis, the outputs from both previous stages are consolidated and visualized to enable comparative analysis.

The outputs consist of structured machine-readable datasets (e.g., CSV files) that contain both raw measurements and

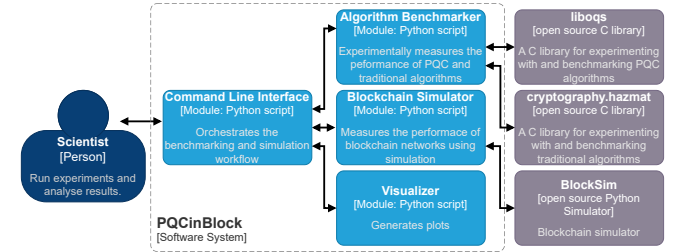


Fig. 2. Architecture of the PQCCinBlock.

aggregated statistics, including mean and standard deviation. These datasets are complemented by graphical visualizations, such as bar charts, which support interpretation and highlight performance trade-offs across algorithms.

B. Implementation

We present **PQCCinBlock**¹, a tool designed to evaluate both traditional and post-quantum cryptographic (PQC) algorithms. The tool is developed with two main objectives: (1) to enable comprehensive comparative analysis of cryptographic algorithms in both isolated and simulated blockchain environments, and (2) to provide extensibility for integrating new cryptographic schemes as they are developed.

Figure 2 illustrates the architecture of **PQCCinBlock**. The Main module receives and validates input parameters and orchestrates the other modules, which operate as described below.

The Algorithm Benchmarker module executes the selected algorithms in *Python*, computing means and standard

¹Source code available at: <https://github.com/conseg/PQCCinBlock>

TABLE III
SYSTEM ENVIRONMENTS.

Machine	CPU	Mem.	OS	Timer Resolution
Laptop ARM	Apple M1	8 GB	macOS Darwin Kernel 24.0.0	40.978193 ns
Laptop x64	Intel Core i7-1360P	32 GB	Ubuntu 22.04.1 LTS Linux Kernel 6.8.0-65-generic	37.980498 ns
Desktop	AMD Ryzen 7 5800X	80 GB	Ubuntu 24.04.2 LTS Linux Kernel 6.8.0-64-generic	49.971276 ns

deviations for key generation, signature creation, and signature verification. It enables the integration of new algorithms and programming languages without requiring modifications to other modules. To add a new algorithm, users create a Python file in the `algorithms` directory describing the cryptographic variants, their security levels, and the functions to measure operational performance. Currently, we use the `liboqs` version 0.12.0 library for post-quantum algorithms and `cryptography` version 45.0.2 for the traditional ECDSA algorithm. Both libraries are wrappers for *C/C++* implementations, enabling direct comparisons between traditional and post-quantum approaches.

The module currently supports the algorithms listed in Table II, including ECDSA, ML-DSA, several variants of SPHINCS+ (*e.g.*, SPHINCS+-SHA-s, SPHINCS+-SHAKE-f), Falcon, Mayo, and multiple implementations of Cross-rsdp and Cross-rsdpg. It is important to note that ML-DSA is equivalent to Dilithium under the nomenclature adopted by NIST in 2024 [16], while Falcon-padded is a variant of Falcon with fixed-length signatures.

The Blockchain Simulator models the behavior of blockchain networks. It leverages performance metrics from the Algorithm Benchmark module to assess the impact of cryptographic algorithms on block verification processes. Currently, we employ `BlockSim` [17], an open-source blockchain simulation framework that captures the behavior of key blockchain layers, including network propagation, consensus mechanisms, and incentive structures. The `PQCinBlock` framework, using the `BlockSim` simulator, currently supports two blockchain models: Bitcoin and Ethereum.

The Visualizer module processes raw output data from the other components, generating plots that enable comparative analysis of algorithm performance across different evaluation scenarios. It currently produces bar plots to display both benchmarking results and blockchain simulation outcomes.

C. Instantiation

The experiments were conducted across multiple hardware configurations (detailed in Table III) to minimize potential biases introduced by specific CPU architectures or operating systems.

Our experimental methodology included comprehensive benchmarking of all available algorithm variants, including nominally distinct but functionally equivalent implementations.

The evaluation framework simulated Bitcoin and an Ethereum-based blockchain environment. To ensure statistical validity, we executed 1,000 warm-up iterations (which were discarded), as well as 10,000 measured executions per algorithm variant and 1,000 simulations. Parameters are listed in Table IV.

TABLE IV
EVALUATION PARAMETERS.

Argument	Value(s)	Description
--runs, -r	10,000	Number of executions of each algorithm.
--warm-up, -wp	1,000	Number of warm-up runs before the main measurement, for performance stabilization.
--levels, -l	{1, 2, 3, 5}	Defines the NIST security levels (1 to 5) of the algorithms to be tested. Can receive multiple values.
--runs-simulator	1,000	Number of simulation runs in <code>BlockSim</code> .
--model	{1, 2}	Bitcoin, Ethereum networks.

IV. EVALUATION RESULTS

We present our results through three sequential components: (*i*) benchmarking of cryptographic algorithms, (*ii*) system-level blockchain simulations, and (*iii*) interpretation of findings, including the identification of methodological constraints.

A. Benchmark of Cryptographic Algorithms

Table V presents the complete benchmark results, including the mean execution time and standard deviation for each algorithm implementation across all available security levels. These metrics were calculated over the specified number of runs for key-pair generation, signing, and verification operations. Due to space constraints, ML-DSA Level 2 results are shown in the column designated for lower levels (1 or 2), as ML-DSA does not provide a Level 1 variant.

The comprehensive results in Table V illustrate the complexity of the study, while cross-machine consistency confirms the reliability of our methodology. Among the higher-cost PQC algorithms, the top performers (ML-DSA and Mayo) were selected for further analysis.

Figure 3 highlights consistent performance patterns across different hardware configurations and security levels. The results confirm the expected trend of increased computational overhead with higher security levels. Notably, the small standard deviations across all measurements indicate statistical reliability despite potential system-level interference, which validates the adequacy of our sample size.

Our analysis shows that ML-DSA outperforms ECDSA in most operations and security levels, except for Level 1 key-pair generation and signing operations. This comparison is particularly significant since ML-DSA's minimum security level (Level 2) exceeds ECDSA's Level 1, making its performance advantage even more relevant. Mayo exhibits comparable or better performance than ECDSA at Levels 1 and 3 on x64 systems. At Level 5, Mayo demonstrates faster verification but slower key generation and signing operations compared to ECDSA.

TABLE V
COMPLETE RESULTS ON THE PERFORMANCE OF CRYPTOGRAPHY ALGORITHMS (MS).

Algorithm	Lower Level (1 or 2)			Level 3			Level 5		
	keypair (mean \pm std)	sign (mean \pm std)	verify (mean \pm std)	keypair (mean \pm std)	sign (mean \pm std)	verify (mean \pm std)	keypair (mean \pm std)	sign (mean \pm std)	verify (mean \pm std)
Laptop ARM									
ECDSA	0.0198 \pm 0.001	0.0441 \pm 0.0021	0.0788 \pm 0.0029	0.2426 \pm 0.0091	0.3758 \pm 0.0122	0.7366 \pm 0.0162	0.2838 \pm 0.0089	0.4973 \pm 0.0157	0.8847 \pm 0.0202
ML-DSA	0.049 \pm 0.0041	0.2113 \pm 0.1409	0.0529 \pm 0.0026	0.0934 \pm 0.0033	0.3425 \pm 0.2338	0.0847 \pm 0.0045	0.1351 \pm 0.0056	0.4295 \pm 0.2668	0.1402 \pm 0.0055
Dilithium	0.0218 \pm 0.0013	0.0653 \pm 0.0407	0.0221 \pm 0.0013	0.0465 \pm 0.0026	0.0979 \pm 0.0604	0.0329 \pm 0.0021	0.0537 \pm 0.0026	0.1195 \pm 0.061	0.0522 \pm 0.0021
Falcon	5.2091 \pm 1.2291	0.155 \pm 0.0043	0.029 \pm 0.0036				16.7976 \pm 4.2397	0.3071 \pm 0.0062	0.0557 \pm 0.0044
Falcon-padded	5.1996 \pm 1.1972	0.1552 \pm 0.0044	0.0286 \pm 0.0022				16.7562 \pm 4.226	0.3082 \pm 0.0102	0.0551 \pm 0.0029
Mayo	0.2576 \pm 0.0033	0.3999 \pm 0.0046	0.0342 \pm 0.0015				0.9739 \pm 0.0082	2.7203 \pm 0.0161	0.379 \pm 0.0045
SPHINCS-SHA-s	39.8194 \pm 4.4966	302.4854 \pm 1.319	0.3056 \pm 0.0144				39.0708 \pm 0.2259	528.3311 \pm 2.7981	0.7282 \pm 0.0197
SPHINCS-SHA-f	0.6223 \pm 0.0089	14.4995 \pm 0.1365	0.8713 \pm 0.0231				0.928 \pm 0.0102	25.3311 \pm 0.178	2.4538 \pm 0.023
SPHINCS-SHAKE-s	73.1857 \pm 0.4665	556.0264 \pm 6.5939	0.5522 \pm 0.0245	108.2966 \pm 0.8138	975.1893 \pm 6.5981	0.8076 \pm 0.0241	72.2639 \pm 0.5518	860.007 \pm 5.8928	1.1941 \pm 0.0326
SPHINCS-SHAKE-f	1.1397 \pm 0.0151	26.6009 \pm 0.2408	1.5859 \pm 0.0047	1.7003 \pm 0.0197	43.8261 \pm 0.3477	2.3626 \pm 0.0443	4.5113 \pm 0.0496	90.6262 \pm 0.7514	2.4171 \pm 0.0523
Cross-rsdp-small	0.0144 \pm 0.001	3.0152 \pm 0.0302	1.7568 \pm 0.0198	0.0306 \pm 0.0014	4.268 \pm 0.0274	2.3046 \pm 0.0197	0.052 \pm 0.0017	6.1769 \pm 0.0642	3.0694 \pm 0.0358
Cross-rsdp-small	0.0075 \pm 0.0011	2.171 \pm 0.0271	1.1833 \pm 0.0156	0.0137 \pm 0.0011	2.7817 \pm 0.0207	1.7868 \pm 0.0157	0.0219 \pm 0.0012	3.7108 \pm 0.0408	2.2536 \pm 0.0261
Cross-rsdp-balanced	0.0141 \pm 0.0009	0.7992 \pm 0.0076	0.4615 \pm 0.0052	0.0306 \pm 0.0013	1.8272 \pm 0.0149	1.0017 \pm 0.0093	0.0527 \pm 0.0018	3.3201 \pm 0.0297	1.7039 \pm 0.0168
Cross-rsdp-balanced	0.0073 \pm 0.0006	0.6097 \pm 0.0059	0.3368 \pm 0.0044	0.0137 \pm 0.0008	0.7664 \pm 0.0071	0.4722 \pm 0.0054	0.0216 \pm 0.0012	1.3359 \pm 0.0111	0.8144 \pm 0.0074
Cross-rsdp-fast	0.0141 \pm 0.0007	0.4544 \pm 0.0131	0.2603 \pm 0.007	0.0306 \pm 0.0013	1.0475 \pm 0.0115	0.6051 \pm 0.0086	0.0517 \pm 0.0014	2.0195 \pm 0.0171	1.1543 \pm 0.0095
Cross-rsdp-fast	0.0073 \pm 0.0007	0.3221 \pm 0.0034	0.1877 \pm 0.0028	0.0136 \pm 0.0008	0.6023 \pm 0.0066	0.3743 \pm 0.006	0.0221 \pm 0.0009	1.1189 \pm 0.0105	0.6675 \pm 0.0068
Laptop x64									
ECDSA	0.012 \pm 0.0009	0.0259 \pm 0.001	0.0574 \pm 0.0014	0.0775 \pm 0.0013	0.1263 \pm 0.0015	0.2512 \pm 0.0024	0.0866 \pm 0.0025	0.1754 \pm 0.0046	0.3126 \pm 0.0081
ML-DSA	0.0193 \pm 0.0009	0.0493 \pm 0.0277	0.0196 \pm 0.0007	0.0322 \pm 0.0011	0.0795 \pm 0.0458	0.0315 \pm 0.001	0.0491 \pm 0.0017	0.0956 \pm 0.0445	0.0479 \pm 0.0016
Dilithium	0.0192 \pm 0.0009	0.0488 \pm 0.0277	0.0193 \pm 0.0009	0.0322 \pm 0.0014	0.0796 \pm 0.0468	0.0315 \pm 0.0011	0.0504 \pm 0.0015	0.0977 \pm 0.0452	0.0493 \pm 0.0014
Falcon	5.8027 \pm 1.5008	0.2039 \pm 0.0034	0.0434 \pm 0.0026				13.2128 \pm 3.3529	0.2944 \pm 0.0059	0.0604 \pm 0.003
Falcon-padded	4.3956 \pm 1.083	0.1555 \pm 0.0058	0.0319 \pm 0.0007				13.1972 \pm 3.311	0.3002 \pm 0.009	0.0592 \pm 0.001
Mayo	0.0289 \pm 0.001	0.063 \pm 0.009	0.0142 \pm 0.0022	0.0528 \pm 0.0008	0.1867 \pm 0.0023	0.0673 \pm 0.0009	0.1188 \pm 0.0017	0.36 \pm 0.0046	0.1245 \pm 0.0017
SPHINCS-SHA-s	17.4697 \pm 0.1948	132.7452 \pm 1.3186	0.1787 \pm 0.0059	26.2132 \pm 0.2847	253.8474 \pm 1.932	0.298 \pm 0.0069	17.4807 \pm 0.1946	231.1655 \pm 1.8035	0.4163 \pm 0.0094
SPHINCS-SHA-f	0.2817 \pm 0.0036	6.537 \pm 0.0702	0.493 \pm 0.0122	0.4189 \pm 0.0048	11.3276 \pm 0.1266	0.7512 \pm 0.0132	1.1024 \pm 0.0127	23.2572 \pm 0.2587	0.7621 \pm 0.0141
SPHINCS-SHAKE-s	36.7059 \pm 0.1882	279.7878 \pm 0.876	0.3461 \pm 0.0108	53.8654 \pm 0.4963	483.193 \pm 1.5473	0.4903 \pm 0.0122	35.6218 \pm 0.1637	423.1682 \pm 1.1481	0.7043 \pm 0.0154
SPHINCS-SHAKE-f	0.577 \pm 0.0062	13.4564 \pm 0.1352	0.9368 \pm 0.0208	0.8483 \pm 0.0059	21.8742 \pm 0.1583	1.3467 \pm 0.0206	2.2406 \pm 0.0109	44.9622 \pm 0.2045	1.3681 \pm 0.022
Cross-rsdp-small	0.0155 \pm 0.0007	2.0538 \pm 0.0168	1.5309 \pm 0.014	0.0295 \pm 0.0008	2.955 \pm 0.0274	2.1288 \pm 0.0233	0.0439 \pm 0.0013	3.9732 \pm 0.0433	2.839 \pm 0.0353
Cross-rsdp-small	0.0086 \pm 0.0006	1.425 \pm 0.014	0.911 \pm 0.0133	0.0146 \pm 0.0008	2.3393 \pm 0.0275	1.4576 \pm 0.017	0.0222 \pm 0.0008	2.9133 \pm 0.0367	1.7825 \pm 0.0241
Cross-rsdp-balanced	0.0145 \pm 0.0011	0.5602 \pm 0.0104	0.3905 \pm 0.0071	0.03 \pm 0.0043	1.2859 \pm 0.0166	0.8724 \pm 0.0093	0.0463 \pm 0.0016	2.148 \pm 0.026	1.4411 \pm 0.018
Cross-rsdp-balanced	0.0082 \pm 0.001	0.4135 \pm 0.0069	0.2599 \pm 0.0024	0.0141 \pm 0.0006	0.6513 \pm 0.0095	0.4012 \pm 0.0094	0.0216 \pm 0.0008	1.0667 \pm 0.0158	0.6573 \pm 0.0088
Cross-rsdp-fast	0.0137 \pm 0.0006	0.337 \pm 0.0084	0.2101 \pm 0.0023	0.0296 \pm 0.0007	0.7728 \pm 0.0087	0.4858 \pm 0.0057	0.0458 \pm 0.001	1.3681 \pm 0.012	0.8397 \pm 0.0076
Cross-rsdp-fast	0.0081 \pm 0.0006	0.2336 \pm 0.0138	0.1457 \pm 0.0095	0.0137 \pm 0.0006	0.5491 \pm 0.0062	0.3446 \pm 0.0039	0.0212 \pm 0.0007	0.8832 \pm 0.0129	0.5626 \pm 0.0088
Desktop									
ECDSA	0.015 \pm 0.001	0.033 \pm 0.0016	0.0615 \pm 0.0019	0.1218 \pm 0.0045	0.1992 \pm 0.0067	0.3977 \pm 0.011	0.1087 \pm 0.0027	0.2243 \pm 0.0042	0.3909 \pm 0.0067
ML-DSA	0.0236 \pm 0.0008	0.0553 \pm 0.0297	0.0226 \pm 0.0006	0.0387 \pm 0.0017	0.0873 \pm 0.0473	0.0368 \pm 0.0014	0.0605 \pm 0.0019	0.1071 \pm 0.0455	0.0578 \pm 0.0017
Dilithium	0.0234 \pm 0.0008	0.0548 \pm 0.0301	0.0225 \pm 0.0006	0.0386 \pm 0.0008	0.086 \pm 0.0459	0.0368 \pm 0.0007	0.0605 \pm 0.0011	0.1086 \pm 0.0467	0.0579 \pm 0.001
Falcon	4.5585 \pm 1.1817	0.1584 \pm 0.0022	0.034 \pm 0.002				13.5104 \pm 3.46	0.3151 \pm 0.0035	0.0653 \pm 0.0029
Falcon-padded	4.5356 \pm 1.1917	0.1619 \pm 0.0021	0.0338 \pm 0.0025				13.4322 \pm 3.3585	0.3197 \pm 0.0078	0.0645 \pm 0.001
Mayo	0.0237 \pm 0.0007	0.0582 \pm 0.0011	0.0133 \pm 0.0004	0.0418 \pm 0.0013	0.1542 \pm 0.0015	0.0473 \pm 0.001	0.0884 \pm 0.0002	0.3045 \pm 0.0031	0.0921 \pm 0.0012
SPHINCS-SHA-s	15.1549 \pm 0.0525	115.2267 \pm 0.2323	0.166 \pm 0.0056	22.1562 \pm 0.1061	212.136 \pm 0.8036	0.278 \pm 0.0066	14.8261 \pm 0.1126	192.8551 \pm 1.4157	0.3829 \pm 0.0077
SPHINCS-SHA-f	0.2407 \pm 0.0033	5.5964 \pm 0.021	0.4355 \pm 0.0083	0.3587 \pm 0.0033	9.5745 \pm 0.0147	0.6604 \pm 0.0083	0.9285 \pm 0.0034	19.4653 \pm 0.0334	0.6719 \pm 0.01
SPHINCS-SHAKE-s	32.1903 \pm 0.2419	245.0352 \pm 1.7179	0.3163 \pm 0.0108	49.5265 \pm 0.3534	444.061 \pm 3.1006	0.4499 \pm 0.0113	29.7797 \pm 0.0936	359.8339 \pm 0.6492	0.6277 \pm 0.0143
SPHINCS-SHAKE-f	0.4978 \pm 0.0061	11.6084 \pm 0.0367	0.8352 \pm 0.0213	0.7429 \pm 0.0038	19.1604 \pm 0.052	1.228 \pm 0.0171	1.887 \pm 0.0123	38.123 \pm 0.0904	1.1994 \pm 0.0206
Cross-rsdp-small	0.0154 \pm 0.0007	1.9686 \pm 0.0071	1.4158 \pm 0.0058	0.0313 \pm 0.0008	2.7865 \pm 0.0118	1.9685 \pm 0.0072	0.0419 \pm 0.0011	3.7086 \pm 0.0116	2.583 \pm 0.0094
Cross-rsdp-small	0.0091 \pm 0.0006	1.3865 \pm 0.0054	0.8851 \pm 0.0041	0.015 \pm 0.0008	2.243 \pm 0.0101	1.4572 \pm 0.0064	0.0216 \pm 0.0007	2.7278 \pm 0.0091	1.6763 \pm 0.005
Cross-rsdp-balanced	0.0151 \pm 0.0009	0.5354 \pm 0.0036	0.3674 \pm 0.0028	0.031 \pm 0.001	1.1966 \pm 0.0044	0.8251 \pm 0.0033	0.0417 \pm 0.0012	1.9548 \pm 0.0068	1.3485 \pm 0.0052
Cross-rsdp-balanced	0.0086 \pm 0.0006	0.3987 \pm 0.0023	0.248 \pm 0.0018	0.0147 \pm 0.0007	0.6246 \pm 0.0025	0.385 \pm 0.001			

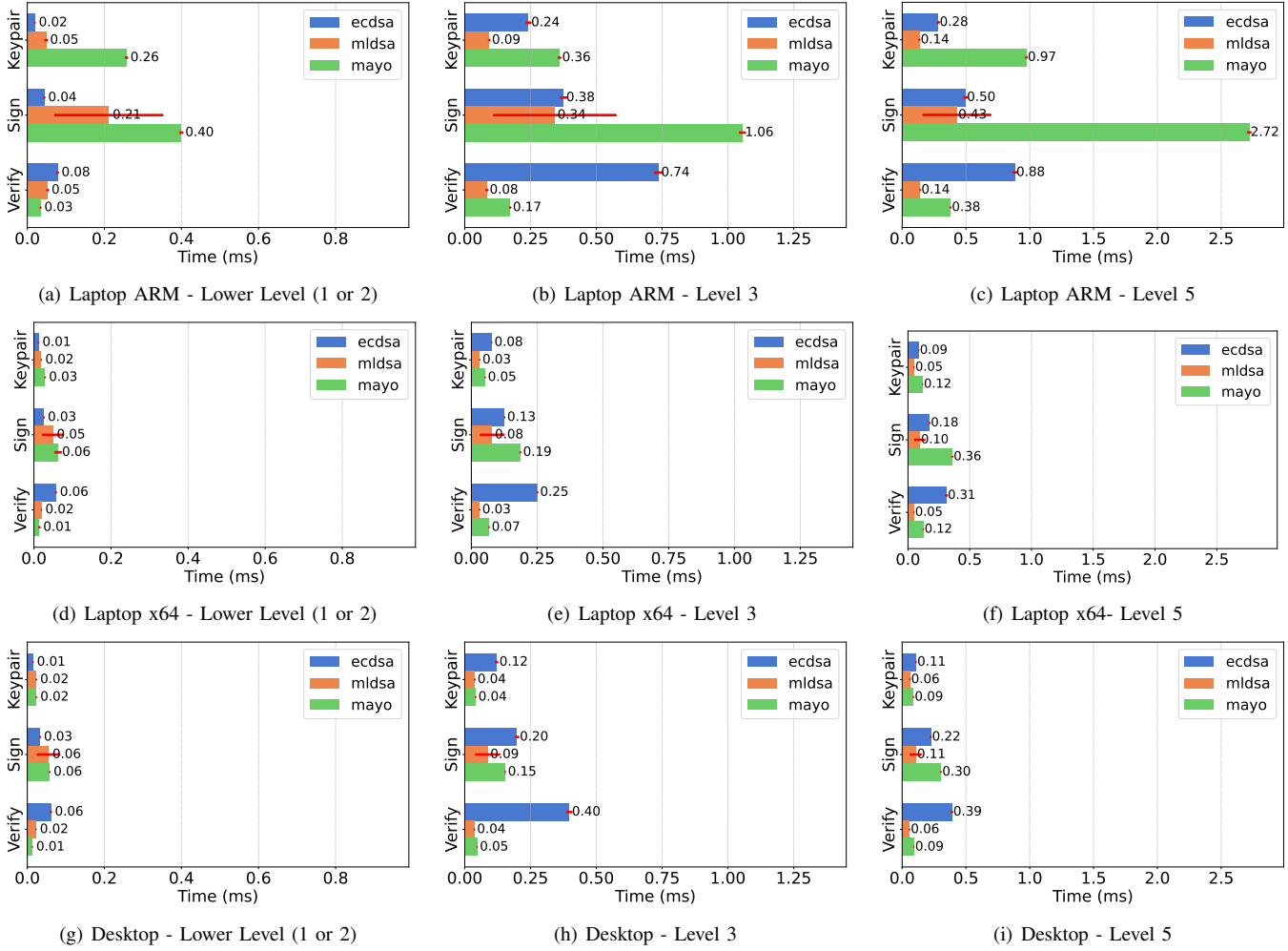


Fig. 3. Benchmarking: Selected Results (Lower Values Indicate Better Results).

algorithms, particularly ML-DSA and Mayo, can be performed smoothly in systems where application performance is the primary requirement. However, migrating to other algorithms, such as SLH-DSA and Cross-rsdp, is not recommended in these scenarios due to performance limitations.

Although this study did not evaluate the sizes of public keys, private keys, and digital signatures, previous works [9], [13], [14] and published standards [3], [4] indicate that PQC-generated keys and signatures are considerably larger than those of ECDSA. Except SLH-DSA, which has the same key size as ECDSA. Systems with storage constraints, including blockchain networks and IoT devices, must balance application security requirements against the capacity to store these larger keys and signatures when deciding which algorithms to adopt.

Moreover, adopting PQC algorithms in blockchains requires considering not only computational performance but also the impact of larger keys and signatures on transaction and block sizes. Larger signatures increase transaction size, reducing the number of transactions per block. Consequently, larger blocks with fewer transactions can elevate latency for consensus or

transaction confirmation, potentially affecting overall network throughput.

D. Limitations

Comparisons with other traditional algorithms, such as RSA, were not conducted in this study. Additionally, discussions on the adoption and potential improvements of key encapsulation mechanisms (KEM) [18] are beyond the scope of this work. Our focus is specifically on processing involving digital signatures, as employed in the most widely used blockchains, including Bitcoin and Ethereum.

Although some proposed solutions explore blockchain applications in IoT contexts [19]–[21], we chose to concentrate our experiments on the most prevalent blockchain systems. Furthermore, BlockSim currently supports only Bitcoin and Ethereum, which are not commonly used in IoT deployments. Evaluating the impact of PQC algorithms in IoT devices remains an avenue for future research.

TABLE VI
COMPLETE RESULTS OF THE BLOCKCHAIN SIMULATIONS (ms).

Algorithm	Laptop ARM verify (mean \pm std)			Laptop x64 verify (mean \pm std)			Desktop verify (mean \pm std)		
	Lower Level	Level 3	Level 5	Lower Level	Level 3	Level 5	Lower Level	Level 3	Level 5
Bitcoin									
ECDSA	136.2845 \pm 2.3648	1273.9468 \pm 22.616	1531.0027 \pm 26.5852	99.2422 \pm 1.7495	434.3056 \pm 8.2095	541.203 \pm 8.8813	106.4078 \pm 2.0004	687.6015 \pm 11.907	676.0999 \pm 12.2533
ML-DSA	91.3405 \pm 1.6492	146.6004 \pm 2.5224	242.2411 \pm 4.3684	33.8754 \pm 0.5687	54.3813 \pm 0.9583	82.9072 \pm 1.3698	39.1121 \pm 0.6682	63.6307 \pm 1.1611	100.0014 \pm 1.7721
Dilithium	38.2409 \pm 0.6844	56.9484 \pm 1.0043	90.3939 \pm 1.5367	33.4214 \pm 0.6072	54.4299 \pm 1.0108	85.3526 \pm 1.4914	38.9487 \pm 0.7239	63.698 \pm 1.1343	100.1268 \pm 1.8287
Falcon	50.221 \pm 0.8659			96.4311 \pm 1.6821			104.4389 \pm 1.8022	58.8385 \pm 1.1036	
Falcon-padded	49.5613 \pm 0.9207			95.3122 \pm 1.7944	55.1643 \pm 0.9526		102.4074 \pm 1.7481	58.4768 \pm 1.0218	
Mayo	59.1631 \pm 1.0231	299.4169 \pm 5.2516		655.7262 \pm 12.0629	24.5113 \pm 0.4112	116.3231 \pm 2.1785	215.494 \pm 3.5414	22.9609 \pm 0.4017	
SPHINCS-SHA-s	528.9003 \pm 9.4844	871.5926 \pm 15.626	1260.301 \pm 22.5475	309.1484 \pm 5.5676	515.6341 \pm 9.228	720.2043 \pm 12.1136	287.0224 \pm 5.2349	481.1766 \pm 8.638	662.8648 \pm 11.1765
SPHINCS-SHA-f	1507.3205 \pm 25.3508	2361.3837 \pm 42.4078	2434.5585 \pm 43.5861	853.0385 \pm 15.3951	1298.8756 \pm 22.9854	1318.8456 \pm 23.0709	753.3344 \pm 14.9031	1141.0721 \pm 20.085	1162.6435 \pm 19.3736
SPHINCS-SHAKE-s	954.4281 \pm 16.8238	1396.1869 \pm 24.1091	2065.4039 \pm 37.0847	599.1115 \pm 10.3477	847.6319 \pm 15.0924	1218.7581 \pm 20.8864	547.3769 \pm 9.5828	777.7835 \pm 13.7176	1086.4028 \pm 18.9974
SPHINCS-SHAKE-f	2745.388 \pm 45.5068	4084.8346 \pm 75.6695	4180.3499 \pm 73.4508	1620.9727 \pm 30.3867	2330.0321 \pm 41.1458	2366.5064 \pm 44.7915	1444.0436 \pm 25.8178	2124.6605 \pm 40.8339	2074.9598 \pm 36.0649
Cross-rsdp-small	3036.4521 \pm 56.3102	3987.9731 \pm 67.4678	5302.8723 \pm 101.464	2648.0999 \pm 47.0922	3683.7922 \pm 64.0329	4917.4178 \pm 90.5952	2447.8821 \pm 46.593	3405.9624 \pm 58.4809	4468.295 \pm 81.5143
Cross-rsdp-small	2048.0467 \pm 34.9935	3090.3061 \pm 56.5592	3897.5645 \pm 72.9742	1575.7796 \pm 27.6206	2522.9822 \pm 44.7467	3083.8917 \pm 52.2752	1531.6611 \pm 25.7086	2522.5871 \pm 43.5081	2900.9881 \pm 50.9739
Cross-rsdp-balanced	797.2513 \pm 14.5664	1732.6422 \pm 33.8118	2947.9559 \pm 53.5516	675.7915 \pm 11.7194	1508.6183 \pm 27.3333	2489.3299 \pm 47.2395	636.0842 \pm 11.019	1427.7683 \pm 24.8086	2331.9637 \pm 43.0868
Cross-rsdp-balanced	582.2241 \pm 10.2936	817.1568 \pm 14.0075	1409.3277 \pm 24.231	449.4047 \pm 7.7085	693.8905 \pm 12.7111	1137.5636 \pm 21.8478	428.8288 \pm 7.5287	666.3342 \pm 11.1477	1068.4216 \pm 18.7796
Cross-rsdp-fast	450.1529 \pm 9.1348	1047.6817 \pm 18.6586	1997.015 \pm 35.2195	363.3275 \pm 6.6688	841.1026 \pm 14.1928	1452.9939 \pm 26.2099	340.7624 \pm 5.5979	788.0883 \pm 14.5187	1373.4859 \pm 23.8799
Cross-rsdp-fast	324.5005 \pm 5.9552	647.3387 \pm 11.9267	1154.7252 \pm 19.8287	252.0224 \pm 4.701	596.4249 \pm 10.2094	973.0883 \pm 18.1496	234.9852 \pm 4.4663	561.3991 \pm 10.1477	897.5819 \pm 15.9627
Ethereum									
ECDSA	10.3491 \pm 0.2384	96.6628 \pm 2.1812	116.0763 \pm 2.6017	7.4872 \pm 0.1458	32.7918 \pm 0.6453	40.8184 \pm 0.7706	8.1537 \pm 0.1449	52.7183 \pm 0.9651	51.8054 \pm 0.9224
ML-DSA	6.9448 \pm 0.1578	11.1379 \pm 0.2465	18.418 \pm 0.4154	2.5527 \pm 0.0491	4.1037 \pm 0.0793	6.2515 \pm 0.1186	2.9991 \pm 0.0547	4.8817 \pm 0.0907	7.6552 \pm 0.1401
Dilithium	2.9024 \pm 0.0643	4.3213 \pm 0.0929	6.8603 \pm 0.1544	2.5226 \pm 0.0514	4.1034 \pm 0.0833	6.427 \pm 0.1325	2.9824 \pm 0.0535	4.8851 \pm 0.0829	7.6745 \pm 0.1331
Falcon	3.8116 \pm 0.0863			7.3194 \pm 0.1698	5.6556 \pm 0.1117	7.8667 \pm 0.1552	4.5113 \pm 0.0813		8.6582 \pm 0.1592
Falcon-padded	3.7618 \pm 0.0863			7.2435 \pm 0.1603	4.1596 \pm 0.0772	7.7213 \pm 0.1537	4.4858 \pm 0.0811		8.5432 \pm 0.1531
Mayo	4.4919 \pm 1.002	22.7227 \pm 0.5212	49.7921 \pm 1.1234	18.454 \pm 0.3668	8.7817 \pm 0.1695	16.2426 \pm 0.3261	1.7588 \pm 0.0314	6.2742 \pm 0.1108	12.2031 \pm 0.222
SPHINCS-SHA-s	40.173 \pm 0.903	66.1663 \pm 1.5228	95.5925 \pm 2.233	23.3252 \pm 0.4343	38.8725 \pm 0.781	54.25 \pm 0.0775	22.0238 \pm 0.3913	36.831 \pm 0.67	50.7323 \pm 0.8998
SPHINCS-SHA-f	114.4394 \pm 2.573	179.4633 \pm 4.022	184.6904 \pm 4.1013	64.2922 \pm 1.2847	97.9234 \pm 1.9218	99.2531 \pm 1.9502	57.7019 \pm 1.0366	87.5299 \pm 1.5782	89.0286 \pm 1.5921
SPHINCS-SHAKE-s	72.6221 \pm 1.6532	105.8964 \pm 2.4491	156.9101 \pm 3.5692	45.1136 \pm 0.9134	63.956 \pm 1.2467	91.8136 \pm 1.7776	41.896 \pm 0.7654	59.6529 \pm 1.0579	83.1413 \pm 1.4885
SPHINCS-SHAKE-f	208.2749 \pm 4.8916	310.2855 \pm 6.8458	317.4644 \pm 7.2003	122.203 \pm 2.3795	175.5756 \pm 3.4583	178.4881 \pm 3.3593	110.7192 \pm 2.0648	162.7238 \pm 3.0224	158.9173 \pm 2.8266
Cross-rsdp-small	230.9886 \pm 4.9499	302.7863 \pm 7.0252	403.1348 \pm 9.0603	199.7076 \pm 4.0614	277.5764 \pm 5.2626	370.2685 \pm 7.317	187.608 \pm 3.4582	260.9108 \pm 4.6804	342.4696 \pm 6.2811
Cross-rsdp-small	155.3068 \pm 3.6172	234.7216 \pm 5.222	295.9017 \pm 7.0679	118.6946 \pm 2.3037	190.0899 \pm 3.675	232.5503 \pm 4.6263	117.2321 \pm 2.1072	193.0565 \pm 3.5995	222.1975 \pm 4.0865
Cross-rsdp-balanced	60.5409 \pm 1.3722	131.6209 \pm 2.9952	224.051 \pm 4.8656	50.9738 \pm 0.978	113.8022 \pm 2.2499	188.1103 \pm 3.7592	48.732 \pm 0.9241	109.3643 \pm 1.8698	178.8018 \pm 3.2693
Cross-rsdp-balanced	44.2783 \pm 0.9875	62.0173 \pm 1.4034	107.04 \pm 2.3375	33.937 \pm 0.6676	52.3021 \pm 1.0433	85.7211 \pm 1.6835	32.8924 \pm 0.5854	51.0591 \pm 0.8984	81.8082 \pm 1.5069
Cross-rsdp-fast	34.1856 \pm 0.7596	79.5323 \pm 1.7342	151.6858 \pm 3.2924	27.3821 \pm 0.5532	63.4258 \pm 1.2638	109.5058 \pm 2.065	26.0865 \pm 0.471	60.2854 \pm 1.1056	105.2215 \pm 1.9187
Cross-rsdp-fast	24.6787 \pm 0.5415	49.2222 \pm 1.0755	87.569 \pm 2.0809	19.0112 \pm 0.3663	44.8927 \pm 0.9238	73.4431 \pm 1.4179	18.0222 \pm 0.3291	43.0699 \pm 0.7775	68.8634 \pm 1.2179

V. CONCLUSION

In this work, we presented a comparison between the performance of traditional algorithms, such as ECDSA, and post-quantum cryptographic (PQC) algorithms, including ML-DSA, Falcon, and SPHINCS+, both in isolation and within blockchain systems. We also introduced a tool that benchmarks the core operations of these algorithms—key generation, signing, and verification—and simulates their impact on blockchain.

Our results indicate that certain PQC algorithms, particularly ML-DSA and Mayo, outperform ECDSA, especially at higher security levels. As expected, performance decreases as security levels increase, reflecting the corresponding rise in computational overhead. These findings suggest that replacing algorithms vulnerable to Shor's algorithm is feasible, provided the effects of larger key and signature sizes on network throughput are considered.

As Future work, we intend to investigate the impact of public key, private key and digital signature sizes on blockchain storage and network traffic, evaluating their implications for system efficiency, scalability, and operational viability. Moreover, the modular architecture of `PQCinBlock` allows the integration of new algorithms, programming languages, and experimental scenarios, enabling the tool to support both traditional and post-quantum digital signature schemes in future studies.

REFERENCES

- [1] P. B. Upama, M. J. H. Faruk, M. Nazim, M. Masum, H. Shahriar, G. Uddin, S. Barzanjeh, S. I. Ahamed, and A. Rahman, “Evolution
- [2] P. W. Shor, “Algorithms for quantum computation: discrete logarithms and factoring,” in *Proceedings of the 35th Annual Symposium on Foundations of Computer Science*, ser. SFCS ’94. USA: IEEE Computer Society, 1994, p. 124–134. [Online]. Available: <https://doi.org/10.1109/SFCS.1994.365700>
- [3] NIST, “Module-lattice-based digital signature standard,” National Institute of Standards and Technology, Tech. Rep. FIPS PUB 204, 2024, disponível em: <https://doi.org/10.6028/NIST.FIPS.204>.
- [4] NIST, “Stateless hash-based digital signature standard,” National Institute of Standards and Technology, Tech. Rep. FIPS PUB 205, 2024, disponível em: <https://doi.org/10.6028/NIST.FIPS.205>.
- [5] P.-A. Fouque, J. Hoffstein, P. Kirchner, V. Lyubashevsky, T. Pörrin, T. Prest, T. Ricosset, G. Seiler, W. Whyte, Z. Zhang *et al.*, “Falcon: Fast-fourier lattice-based compact signatures over ntru,” *Submission to the NIST’s post-quantum cryptography standardization process*, vol. 36, no. 5, pp. 1–75, 2018.
- [6] M. Baldi, A. Barenghi, S. Bitzer, P. Karl, F. Manganelli, A. Pavoni, G. Pelosi, P. Santini, J. Schupp, F. Slaughter *et al.*, “Codes and restricted objects signature scheme,” *Submission to the NIST Post-Quantum Cryptography Standardization Process. Algorithm Specifications and Supporting Documentation, Version*, 2025.
- [7] W. Beullens, “Mayo: practical post-quantum signatures from oil-and-vinegar maps,” in *International Conference on Selected Areas in Cryptography*. Springer, 2021, pp. 355–376.
- [8] Z. Yang, H. Alfauri, B. Farkiani, R. Jain, R. D. Pietro, and A. Erbad, “A survey and comparison of post-quantum and quantum blockchains,” *Commun. Surveys Tuts.*, vol. 26, no. 2, p. 967–1002, Apr. 2024. [Online]. Available: <https://doi.org/10.1109/COMST.2023.3325761>
- [9] P. Juaristi, I. Agudo, R. Rios, and L. Ricci, “Benchmarking post-quantum cryptography in ethereum-based blockchains,” in *Computer Security. ESORICS 2024 International Workshops*. Cham: Springer Nature Switzerland, 2025, pp. 340–353.
- [10] M. I. García-Cid, R. Martín, D. Domingo, L. Ortiz, and V. Martín, “Comparative evaluation of quantum-resistant digital signatures,” in *2024*

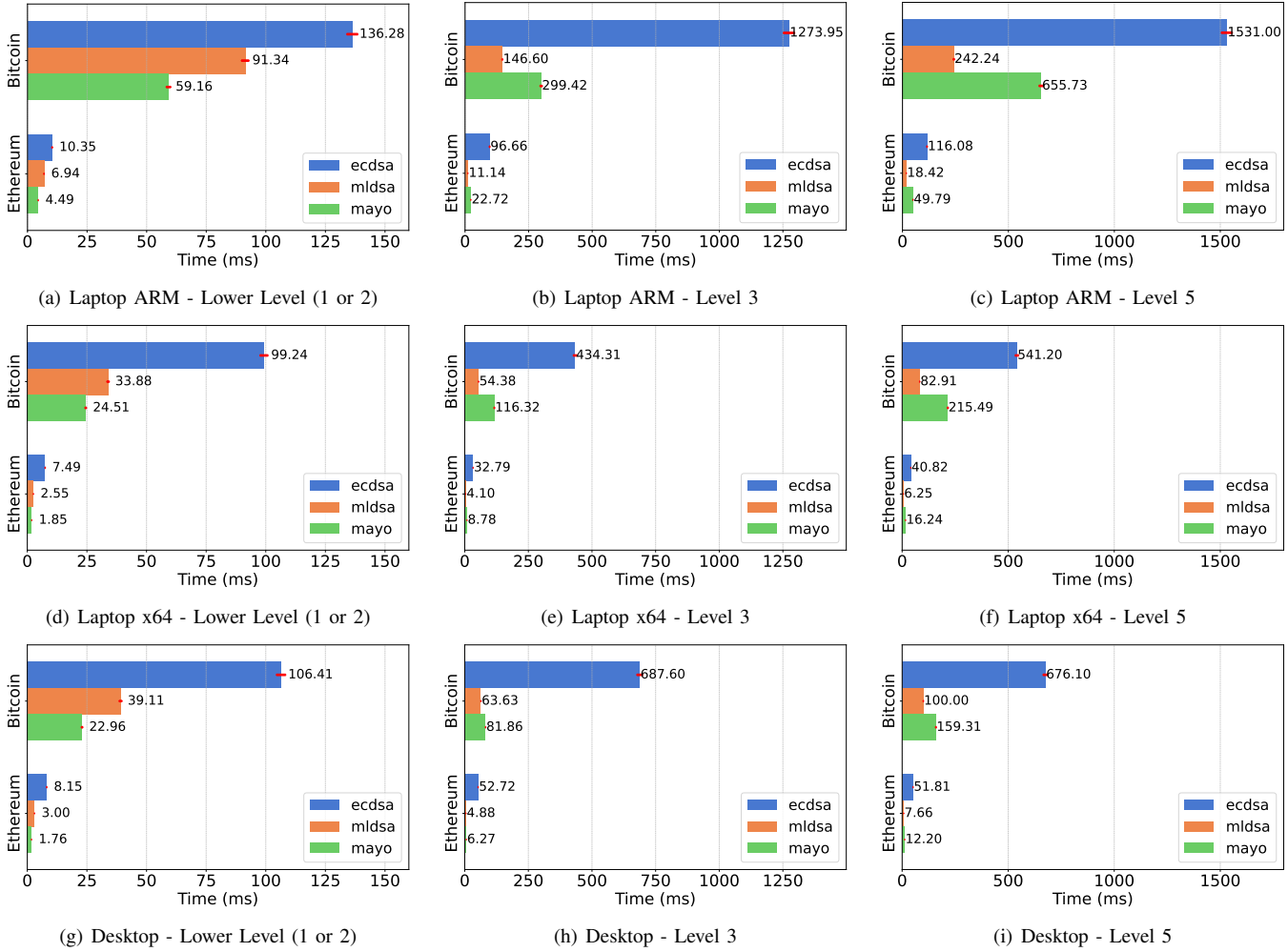


Fig. 4. Main Simulation Results (Lower Values Indicate Better Results).

International Conference on Quantum Communications, Networking, and Computing (QCNC), 2024, pp. 226–230.

- [11] B. Lomc, A. Aubry, H. Bakhti, M. Christofi, and H. A. Mehrez, “Feasibility and benchmarking of post-quantum cryptography in the cooperative its ecosystem,” in *2023 IEEE Vehicular Networking Conference (VNC)*, 2023, pp. 215–222.
- [12] E. D. Demir, B. Bilgin, and M. C. Onbasli, “Performance analysis and industry deployment of post-quantum cryptography algorithms,” 2025, preprint arXiv:2503.12952 [cs.CR]. [Online]. Available: <https://arxiv.org/abs/2503.12952>
- [13] D. Commey, B. Appiah, G. S. Klogo, W. Bagyl-Bac, and J. D. Gadze, “Performance analysis and deployment considerations of post-quantum cryptography for consumer electronics,” 2025, preprint arXiv:2505.02239 [cs.CR]. [Online]. Available: <https://arxiv.org/abs/2505.02239>
- [14] G. Fitzgibbon and C. Ottaviani, “Constrained device performance benchmarking with the implementation of post-quantum cryptography,” *Cryptography*, vol. 8, no. 2, 2024. [Online]. Available: <https://www.mdpi.com/2410-387X/8/2/21>
- [15] NIST, “Call for proposals for public-key cryptographic algorithms,” National Institute of Standards and Technology, Gaithersburg, MD, Federal Register Notice Vol. 81, No. 241, pp. 93915-93918, Dec. 2016. [Online]. Available: <https://csrc.nist.gov/CSRC/media/Projects/Post-Quantum-Cryptography/documents/call-for-proposals-final-dec-2016.pdf>
- [16] NIST, “Nist releases first 3 finalized post-quantum encryption standards,” Aug. 2024, disponível em: <https://www.nist.gov/news-events/news/2024/08/nist-releases-first-3-finalized-post-quantum-encryption-standards>.
- [17] M. Alharby and A. van Moorsel, “Blocksim: An extensible simulation tool for blockchain systems,” *Frontiers in Blockchain*, vol. Volume 3 - 2020, 2020. [Online]. Available: <https://www.frontiersin.org/journals/blockchain/articles/10.3389/fbloc.2020.00028>
- [18] J. Yu, Y. Ding, Y. Guo, K. Kotani, and H. Sato, “Inj-kyber: Enhancing crystals-kyber with information injection within a bio-kem framework,” in *2023 IEEE 22nd International Conference on Trust, Security and Privacy in Computing and Communications (TrustCom)* 2023, pp. 1639–1644.
- [19] A. Dorri, S. S. Kanhere, and R. Jurdak, “Towards an optimized blockchain for iot,” in *Proceedings of the second international conference on Internet-of-Things design and implementation*, 2017, pp. 173–178.
- [20] R. C. Lunardi, R. A. Michelin, H. C. Nunes, C. V. Neu, A. F. Zorzo, and S. S. Kanhere, “Consensus algorithms on appendable-block blockchains: Impact and security analysis,” *Mobile Networks and Applications*, vol. 27, no. 4, pp. 1408–1420, 2022.
- [21] C. Hou, W. Yang, Y. Wang, Z. Zhang, S. Chen, and B. Li, “A multi-blockchain based anonymous cross-domain authentication scheme for industrial internet of things,” in *2024 IEEE 23rd International Conference on Trust, Security and Privacy in Computing and Communications (TrustCom)*, 2024, pp. 1125–1134.